

## BUSBAR OPTIMIZATION USING CELL STABILITY CRITERIA AND ITS IMPACT ON CELL PERFORMANCE

Jacques Antille, René von Kaenel

Alusuisse Technology & Management Ltd.  
Technology Center  
CH-3965 Chippis, Switzerland

### Abstract

The maximum current at which an aluminum reduction cell can be operated is limited by a number of factors. In order to maintain an acceptable heat balance, the anode cathode distance must be reduced when the current is increased. This tends to make the cell unstable or noisy, which leads to lower current efficiency and increased energy consumption. The busbar configuration has a very significant effect on cell stability. It can be altered to improve stability, so that the current can be safely increased. A powerful mathematical model for predicting cell stability has been developed, and used for optimizing busbar systems in two operating smelters. The model predictions and the practical results are presented and discussed.

### Introduction

#### **General considerations**

All smelters aim at the same technical goal, i.e. to achieve at one and the same time the highest possible current efficiency, productivity in tpy per man and the lowest specific energy consumption. They also try to maximize annual tonnage by operating the line at the maximum current. The extent to which the current can be increased depends of course on the available energy but it also depends very much on the technology of the aluminum reduction cells. One essential aspect of that technology

is the arrangement of the busbars. This paper discusses the effects of modifying the busbars in two different plants, SØRAL and ISAL.

The SØRAL smelter (Sør-Norge Aluminium A/S, Husnes, Norway) was first built in 1965 using ALUSUISSE end-to-end pots with pre-baked anode technology and operated at 105 kA with crust breaking from the side. Two lines were built, each with 160 cells, giving a production capacity of 78'000 tons per year at that time. Between 1990 and 1996 the lines were modernized by introducing modern pot controllers, point feeders, a new type of cathode and by making minor modifications to the busbars. The combined effect of these changes was to boost the current from 105 kA to 125 kA, at the same time increasing the current efficiency from 90% to 93.5%. Using mathematical modeling, further busbar modifications were designed with the aim of increasing the current as far as possible. Ten cells were modified for testing. After these had been operated at up to 140 kA for more than two years with a proven current efficiency of over 94%, the plant decided to carry out the same modifications to the first of the two lines. This busbar configuration is named "SØRAL 2000" in order to distinguish it from the "Standard busbar" system. More details concerning the implementation and results can be found in reference [1].

The ISAL smelter (Icelandic Aluminium Co. Ltd. Straumsvík, Iceland) was first built in 1969, with two lines using SØRAL technology. When a third line was added in 1997, it was decided to use the same anode rodding plant and the same cathode shell and operating vehicles. This required that the same type of

technology be used. However, the busbars could be designed from scratch, and a new busbar configuration was designed using Alusuisse numerical modeling tools. This configuration is called “ISAL line-3”. The cells are presently operating at 136 kA due to energy limitations, but are capable of 150 kA.

This paper discusses the analytical tools needed for predicting optimal busbar configurations and the effect on production of these improved configurations.

**The Physical Problem**

Increasing the current in an aluminum reduction cell leads to many different and interacting effects [2]. When the magnetohydrodynamic effects become predominant, or in other words when the forces induced in the liquid metal by the interaction of the magnetic field due to the external busbars with the current flowing in it become too strong, oscillations of the metal surface contour can take place. These oscillations define the limit of stable operation of the cell. From an operational point of view, the cell stability limit can be regarded as the maximum tolerable fluctuation of the cell voltage about its steady-state value (also known as the *noise level*). In order to calculate the cell stability we need first to compute the cell steady state, and then determine the effect on the cell behavior of small perturbations in certain of the operating parameters. The calculation of the cell steady state must be especially accurate, as all steady state values influence the effects of any perturbation [3].

As an example let us consider the determination of the magnetic field. Without going into details of the theory [4], we know that the magnetic field and the current density in the metal have a determining influence on the cell stability limit. The current density, which depends on the magnetic field gradient, can be easily calculated once the magnetic field is known ; it is therefore very important to be able to calculate the steady magnetic field precisely. Figures 1 and 2 describe the calculated and measured magnetic field for two end to end cells in ISAL’s line 3. Figure 1 shows the vertical component ( $B_z$ ) of the induction magnetic field ten centimeters above the carbon cathode inside the liquid metal in front of each anode along the long side of the cell. Figure 2 shows the horizontal component parallel to the long axis at points along the short side of the cell. Round and square spots represent measurements at the two cells. The solid line shows the result of calculations when magnetic effects due to the steel parts of the cell are taken into account and the broken lines the results when they are neglected. The agreement between calculations and the measurements on the two cells is quite good. It is clear that ferromagnetic effects cannot safely be neglected.

**Cell stability diagram**

The determination of the cell stability limit consists in solving a new set of equations resulting from applying a perturbation method to the steady state solution. Details concerning the method can be found in [4,5,6,7,8,9]. Each quantity such as velocity field components, magnetic field components, pressure, metal upheaval, electrical field, and so on is written as a superposition of the stationary solution plus a time-dependent solution. All quantities are introduced into the basic equations (The Maxwell equation, Ohms law, the continuity equation, etc.). These equations take all of the following aspects into consideration:

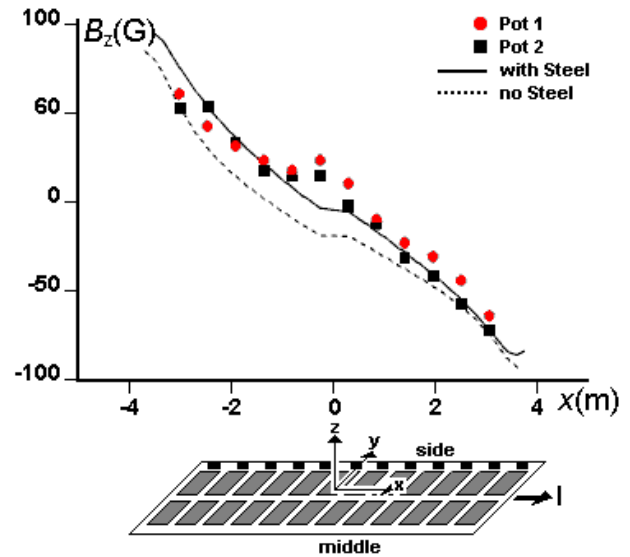


Figure 1: Measured and calculated vertical components of the induction magnetic field ( $B_z$ ) on the long side of the cell

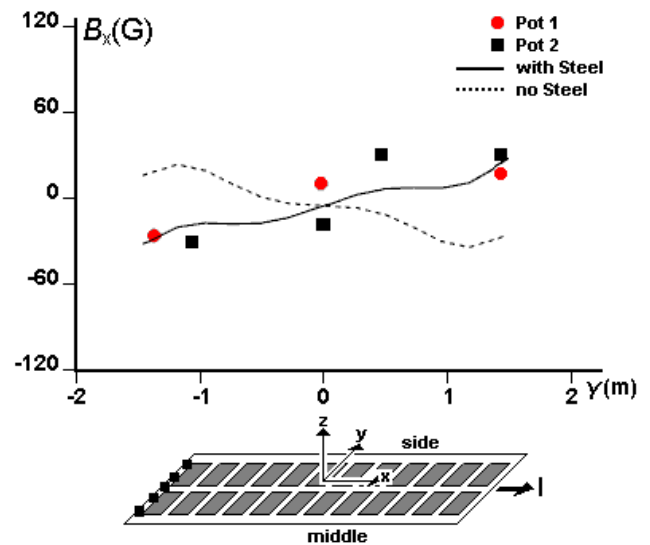


Figure 2: Measured and calculated horizontal components of the induction magnetic field ( $B_x$ ) on the short side of the cell

- three dimensions
- ledge shape and cell cavity shape
- velocity fields in both fluids
- deformed shape of the metal-bath interface
- liquid bath around the anodes

The stationary solution being known, this leads to a new set of equations whose mathematical solution is far from straightforward [4] ; special software was written to implement that solution.

Figure 3 shows a typical stability diagram depicting the resulting eigenfrequencies in the complex plane, with the imaginary part on the y-axis and the real part on the x-axis. The angular velocity  $\omega$  of the wave is plotted on the real axis. From this one can determine the wave frequency and period ( $f = \omega/2\pi$ ,  $T=1/f$ , where  $f$ = frequency,  $T$ = period). In this example the longest wave has a period of 88 seconds and the shortest, 17 seconds. The imaginary part is the stability criterion. When all lines (one line per eigenfrequency) stay above  $-0.6 \cdot 10^{-2} \text{ s}^{-1}$  then the cell is stable. This value of the stability limit has been determined by comparing the stability diagram to the measured noise level of cells in operation. It represents the implicit damping factor due to the fluid viscosity and turbulence.

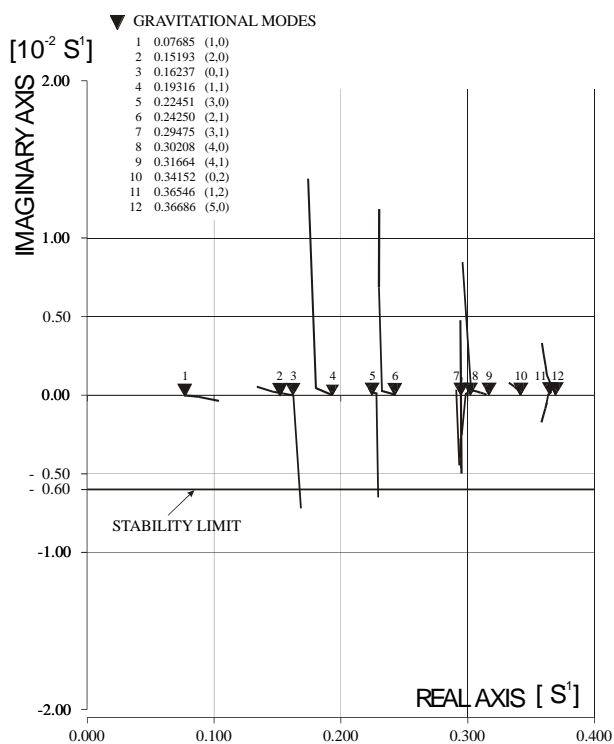


Figure 3: Cell Stability Diagram for the “Standard busbar” system

The analysis starts assuming no current in the cell. In the absence of current the eigenfrequencies are called the gravitational modes. The current is steadily increased and the resulting lines move in the complex plane; some modes remain stable, whereas others may tend towards lower minimum values as the current is increased. The stability limit can be analyzed as a function of maximum current, minimum interpolar distance, minimum metal level and so on. If even only one line (one eigenfrequency) falls below the critical value of  $-0.6 \cdot 10^{-2} \text{ s}^{-1}$ , the cell oscillates and corrective action must be taken. In this example, two modes are unstable when the current is above 135 kA. While the current was increased, the anode cathode distance was reduced in such a way that the cell heat losses were kept unchanged.

If, at the current and voltage at which we wish to operate, the cell stability diagram has one or more lines below the stability limit, then some form of corrective action is essential. One possible corrective action might be to increase the ACD but this is normally undesirable due to the consequent increased demand for

energy. It may be better to modify the busbar configuration. In the next section we examine the effect of such modifications.

## Effects of busbar optimization on cell performance

### Busbar configurations and cell stability

The SØRAL and ISAL smelters both use the same cell technology. The cell stability limit with the Standard busbar system is close to 135 kA, as shown in figure 3. In order to increase the production capacity at SØRAL, it was decided to modify the existing busbar system. Three busbars were added under the cell in order to improve the magnetohydrodynamic state of the cell. An engineering solution was found whereby the new busbars could be built into the cradles under the cell and welded to the existing busbars. The new busbars were designed in such a way that the modification could be carried out with a current interruption of only a few minutes per cell, which is a very important practical advantage in an operating potline. More details concerning the project are given in reference [1]. At ISAL a production increase of 60'000 tpy was planned. When in 1997 a third line was built based on the same cell technology, there were relatively few constraints on the design of the busbar layout, so it proved possible to improve on the layout used at SØRAL. Two raisers were installed at each end of the cell. Figure 4 shows line 3 of EPT-15 cells at ISAL.

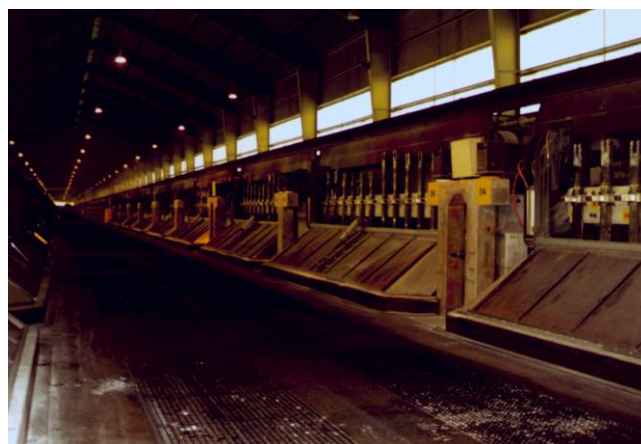


Figure 4: Overview of line 3 of EPT-15 cells at ISAL

Figure 5 shows schematically the corresponding busbar layout.

Figure 6 shows the three busbar arrangements seen from above:

- The Standard busbar arrangement of EPT 12 cell has 40 collector bars. In this configuration 32 collector bars, carrying 80% of total current, are led to the entry of the next cell.
- The “SØRAL 2000” arrangement leads 26 collector bars, carrying 65% of total current, to the entry of the next cell and 6 collector bars to the other end of the cell, under the cell, inside the cradles.
- The “ISAL line-3” arrangement leads 30 collector bars, carrying 75% of total current, to the entry of the next cell and there are two risers at each end.

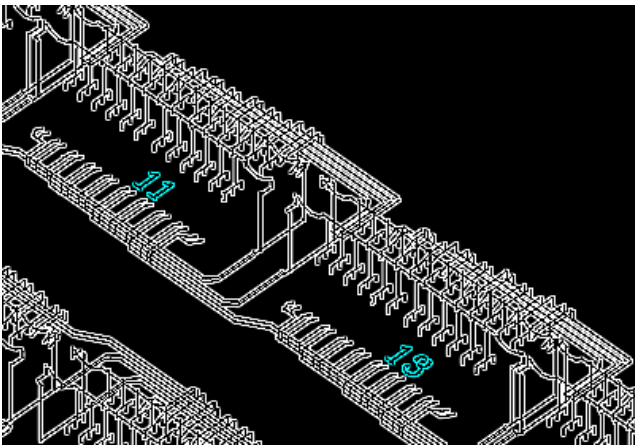
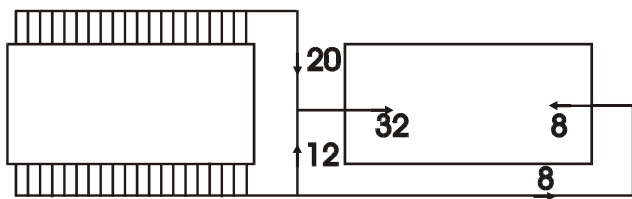
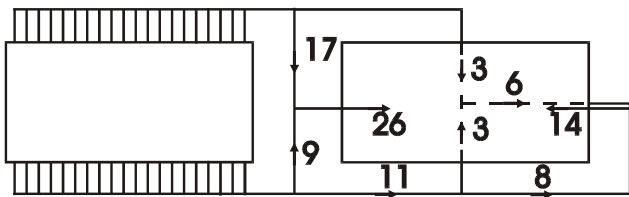


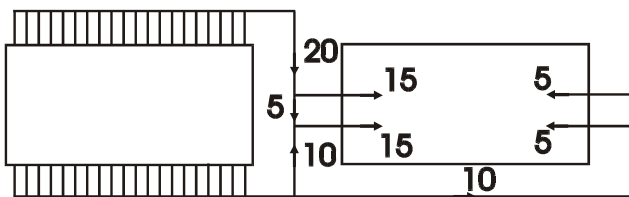
Figure 5: Schematic view of the EPT 15 cell busbar layout at ISAL line 3



EPT12: STANDARD CELL



SORAL 2000



ISAL-LINE3

Figure 6: The three busbar configurations

The effects of these busbar modifications are best seen in the stability diagram. Figure 7 shows the stability diagram for the ISAL line-3 busbar configuration up to 135 kA. The lowest imaginary value is equal to  $-0.08 \cdot 10^{-2}$ , whereas for the Standard busbar configuration it is  $-0.65 \cdot 10^{-2}$  at 135 kA. In other words the cell is much more stable with the ISAL line-3 busbar configuration. This means that the current can further be

increased and the anode cathode distance decreased before reaching the cell stability limit. When operated at 135 kA, it also means that the cell will accept more perturbations such as badly set anodes, ridge and so on, before oscillating.

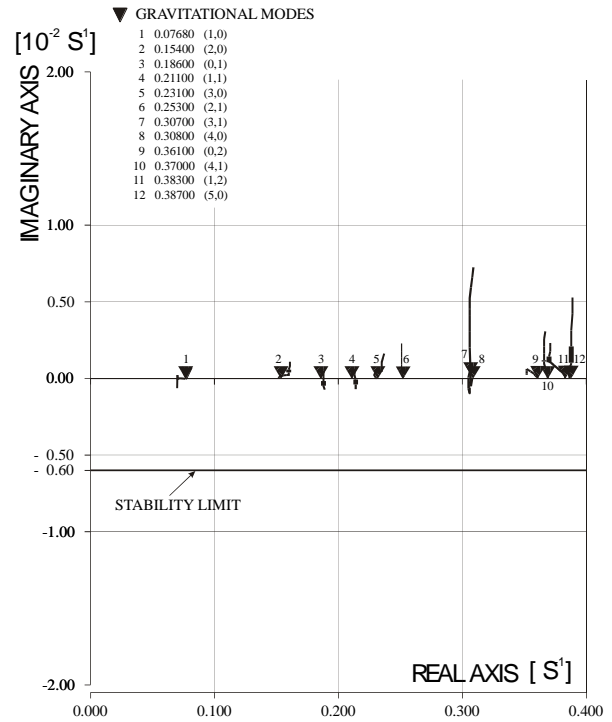


Figure 7: Stability diagram for ISAL line-3 busbar system up to 135 kA

Another way of presenting the results consists in showing the most critical mode (the lowest line in the stability diagram) as a function of the current increase. Figure 8 plots the absolute value of the lowest imaginary part of all eigenfrequencies (often referred to as *growth factor*) as a function of line current for the three busbar configurations. In this representation the stability limit is reached when the line are above  $0.6 \cdot 10^{-2} \text{ s}^{-1}$ .

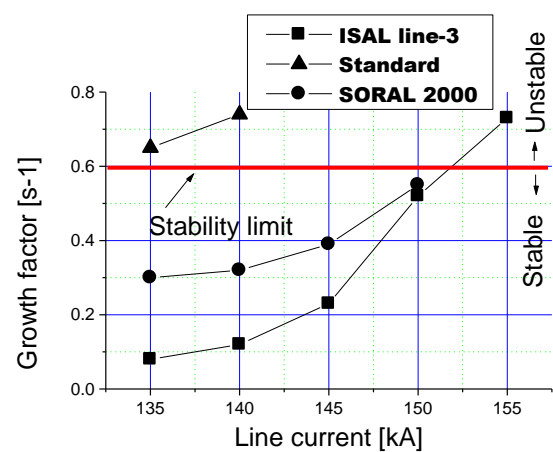


Figure 8: Growth factor for the three busbar configurations

Both the modified busbar configurations, ISAL line-3 and SØRAL 2000, offer a margin of stability at 150 kA, whereas the Standard busbar system becomes critical somewhat below 135 kA. When the ten experimental cells were run at 135 kA in the Standard busbar configuration the level of noise was unacceptable, confirming the predictions of the model.

Comparison of the three busbar configurations using steady-state analysis alone

It is of considerable interest to note that the steady state solutions do not change very much with the new busbar systems. Figure 9 shows the three components of the induction magnetic field at metal level for both the Standard and ISAL line-3 busbar configuration at the edge of the anodes on the long side of the cell. No significant difference is apparent.

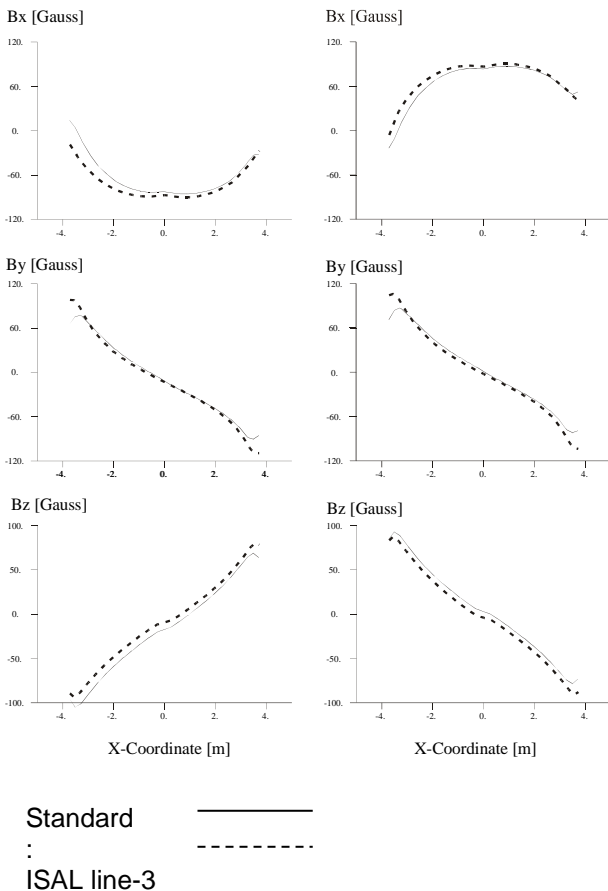


Figure 9: Components of the induction magnetic field for the Standard and ISAL line-3 busbar configurations on the long side of the cell

The limit of stability of a cell is still often reported as depending on the vertical component of the magnetic field in the metal. This statement remains as significant nowadays as when first presented in 1977 [10]. Cell stability however also depends to a significant degree, on many other parameters such as the gradient of the magnetic field, the velocity fields, the ledge shape, the channel

shape (liquid around the anodes). It is the global cell geometry and stationary solution that defines the stability limit. Unfortunately there is no way of deriving a simple explicit formula on the basis of the steady state solution [11].

Since no conclusions can be derived from the magnetic field, it may be interesting to analyze the metal surface contour and the metal velocity field. Table 1 shows the evolution of the mean velocity field in the metal  $\langle V_m \rangle$  and the range of vertical fluctuation of the metal surface contour ( $\Delta h$ ). The reference is the Standard busbar system at 135 kA, i.e. for this configuration  $\langle V_m \rangle$  and  $\Delta h$  are taken to be 100%, corresponding to critical stability. The mean velocity field is smaller, certainly, as is the difference between high and low points on the metal surface contour for the modified busbars; but it is far from clear that the modified pots would be stable even beyond 150 kA. Indeed, the modified pots appear to become unstable just below 140 kA.

If we had only been able to carry out an analysis of the steady state of the pots with the modified busbars, we could not have concluded that the cell might be operated at 150 kA.

Steady state analysis is clearly quite inadequate for predicting cell stability limits.

		135 [kA]	140 [kA]	145 [kA]	150 [kA]
Standard	$\langle V_m \rangle$	100%	107%	114%	120%
Standard	$\Delta h$	100%	110%	124%	127%
SØRAL 2000	$\langle V_m \rangle$	90%	97%	102%	108%
SØRAL 2000	$\Delta h$	82%	90%	100%	106%
ISAL Line-3	$\langle V_m \rangle$	94%	98%	104%	109%
ISAL Line-3	$\Delta h$	91%	96%	103%	113%

$\langle V_m \rangle$  = Mean velocity field in the liquid metal  
 $\Delta h$  = Max – Min of metal surface contour level

Table 1: Evolution of Mean Velocity Field in Metal and Metal Surface Contour

Results and Conclusions

**Results**

Ten test cells at SØRAL were modified according to the model predictions, and operated for two years with higher current. Following this, the same modification is being made to the existing lines and the current increased accordingly. Figure 10 shows how the mean current has increased over the last few years, for the test cells and for the two lines.

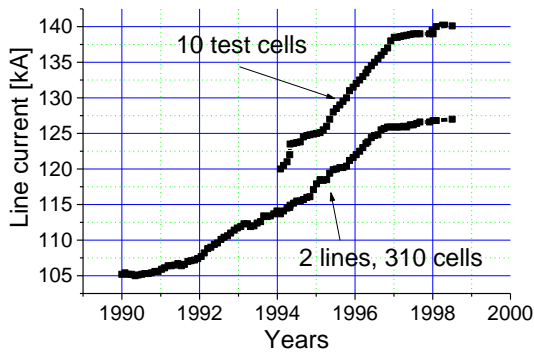


Figure 10: Mean current increase for 10 test cells and two lines (160 cell/line)

As a result of the busbar modifications the following improvements can be achieved in production (Table 2):

Current [kA]	Current efficiency [%]	Production [%]
130	93.5	100.0
140	94.5	108.8
145	94.5	112.7
150	94.5	116.6

Table 2: Increased production due to busbar modifications

The respective modifications to the busbar configuration permit an increase of production of up to 16% at both SØRAL and ISAL. Moreover, not only is this achieved without sacrificing current efficiency, there is even a small improvement. The advantage of the ISAL design is seen in Fig. 7 : although the stability margin is the same as SØRAL when operating at 150kA, it becomes significantly wider at lower levels of current.

### Conclusions

Powerful software for analyzing cell stability was developed. It is fully three dimensional and take into account the cell cavity, ledge shape, deformed shape of the metal-bath interface, velocity fields in both fluids and liquid bath around the anodes. Conventional steady state analysis is necessary for designing a satisfactory reduction cell. However, the conventional analysis is unduly conservative in estimating the stability limits of the cell, because there is no simple stability criterion. Three significantly different busbar configurations appear to have only slightly different steady state solutions. In contrast, when cell stability is analyzed by using a sophisticated stability model, the stability limits can be reliably and accurately estimated. In the case of the three different busbar configurations, such an analysis shows differences in the stability margins offering substantial economic advantages. In practice, it justified investment in modifying the existing lines, and results in important increased production.

### Acknowledgments

The authors wish to acknowledge their debt to the management and engineering teams from the plants and ALESA Ltd. for all efforts that were necessary to lead the two projects to a success as well as to Jean Descloux, Michel Flück and Michel Romerio for the development of the cell stability theory.

### References

- [1] T. Johanson, H.P. Lange, R. von Kaenel, "Productivity Increase at SØRAL Smelter", To be printed in *Light Metals 1999*
- [2] J.P. Antille, M. Givord, Y. Krähenbühl, R. Von Kaenel, "Effects of Current Increase on Aluminium Reduction Cell", *Light Metals 1995*, edited by W. Evans, pp. 315-321
- [3] J. Descloux, M. Flück, M.V. Romerio, "Modeling for Instabilities in Hall-Heroult Cells: Mathematical and Numerical Aspects", *Magneto hydrodynamics in Progress Metallurgy, Light Metals 1992*, Ed. by E.R. Cutshall, pp 1195-1198
- [4] J. Descloux, M. Flück, M.V. Romerio, "Spectral Aspects of an Industrial Problem" *Spectral analysis of complex structure*, Ed Hermann Paris coordinator E. Sanchez Palencia 1995, pp 17-33
- [5] M.V. Romerio, J. Descloux, M. Flück, "Linear Stability of Electrolysis Cells Parts I,II", EPFL, DMA, November 1990
- [6] M.V. Romerio, J. Descloux, M. Flück, "Stability Analysis of an Electrolytic Cell for Aluminium Production by a Perturbation Method Parts I,II", EPFL, DMA, Sept. 1991
- [7] J. Descloux, Y. Jaccard, M.V. Romerio, "Stability in Aluminium Reduction Cells: A Spectral Problem Solved by an Iterative Procedure", *Light Metals 1994*, pp 275-281. Ed. U. Manweiler.
- [8] M. Segatz and C. Droste "Analysis of Magneto hydrodynamic Instabilities in Aluminium Reduction Cells", *Light Metals 1994*, pp 313-322., Ed. U. Manweiler.
- [9] R. von Kaenel, J. Antille, "On the Stability of Alumina Reduction Cells". *Fifth Australasian Aluminium Smelter Conference, 1995, Sydney, Australia*, Ed. B. Welch & M. Skyllas Kazacos, pp 530-544
- [10] T. Sele "Instabilities of the Metal Surface in Electrolytic Cells", *Light Metals 1977*, Ed. by K.B. Higbie, pp 7-24, Volume 1
- [11] J. Descloux, M. Flück, M.V. Romerio, "Modelling of the Stability of Aluminium electrolysis cell", *Non linear partial differential equations and their applications. College de France, Seminaire Volume XIII*, Ed. Longman 1998 pp 117-133